Supplemental material of "Floquet multi-Weyl points in crossing-nodal-line semimetals"

Zhongbo Yan[1] and Zhong Wang[1,2]

[1]*Institute for Advanced Study, Tsinghua University, Beijing, China, 100084*
[2]*Collaborative Innovation Center of Quantum Matter, Beijing 100871, China*

(Dated: July 11, 2017)

This supplemental material contains: (i) The derivation of the effective Floquet Hamiltonian for the type-II crossing model. (ii) Floquet Weyl points in crossing-nodal-line semimetals with cubic symmetry. (iii) Surface state evolution. (vi) Effect of spin-orbit coupling. (v) Experimental estimation.

I. DERIVATION OF THE EFFECTIVE FLOQUET HAMILTONIAN FOR THE TYPE-II CROSSING MODEL

The starting Hamiltonian is

$$H(\mathbf{k}) = [m - B(k_x^2 + k_y^2) + Bk_z^2]\tau_x + \lambda k_y k_z \tau_z. \tag{1}$$

We consider an incident light in the direction $\mathbf{n} = (\cos\phi\sin\theta, \sin\phi\sin\theta, \cos\theta)$. The vector potential of the light is $\mathbf{A}(t) = A_0(\cos(\omega t)\mathbf{e}_1 + \eta\sin(\omega t)\mathbf{e}_2)$, with $\eta = \pm 1$ corresponding to the right-handed and left-handed circularly polarized light, respectively. Here, $\mathbf{e}_1 = (\sin\phi, -\cos\phi, 0)$ and $\mathbf{e}_2 = (\cos\phi\cos\theta, \sin\phi\cos\theta, -\sin\theta)$ are two vectors perpendicular to $\mathbf{n}$, satisfying $\mathbf{e}_1 \cdot \mathbf{e}_2 = 0$.

The electromagnetic coupling is given by $H(\mathbf{k}) \to H(\mathbf{k} + e\mathbf{A}(t))$. The full Hamiltonian is time-periodic, therefore, it can be expanded as $H(t, \mathbf{k}) = \sum_n H_n(\mathbf{k})e^{in\omega t}$ with

$$\begin{aligned}
H_0(\mathbf{k}) &= [m(\theta) - B(k_x^2 + k_y^2) + Bk_z^2]\tau_x + (\lambda k_y k_z - 2D_1)\tau_z, \\
H_{\pm 1}(\mathbf{k}) &= -BeA_0[(\sin\phi k_x - \cos\phi k_y) \\
&\quad \mp i\eta(\cos\phi\cos\theta k_x + \sin\phi\cos\theta k_y + \sin\theta k_z)]\tau_x \\
&\quad -\lambda eA_0[\cos\phi k_z \pm i\eta(\sin\phi\cos\theta k_z - \sin\theta k_y)]\tau_z/2, \\
H_{\pm 2}(\mathbf{k}) &= D_0\tau_x + (D_1 \mp i\eta D_2)\tau_z,
\end{aligned} \tag{2}$$

where $m(\theta) = m - Be^2A_0^2\cos^2\theta$, and $D_0 = -Be^2A_0^2\sin^2\theta/2$, $D_1 = \lambda e^2A_0^2\sin\phi\cos\theta\sin\theta/4$, and $D_2 = \lambda e^2A_0^2\cos\phi\sin\theta/4$.

When ω is in the off-resonance regime, the system is well described by an effective time-independent Hamiltonian, which reads

$$\begin{aligned}
H_{\text{eff}}(\mathbf{k}) &= H_0 + \sum_{n\geq 1}\frac{[H_{+n}, H_{-n}]}{n\omega} + O(\frac{1}{\omega^2}) \\
&= [m(\theta) - B(k_x^2 + k_y^2) + Bk_z^2]\tau_x + (\lambda k_y k_z - 2D_1)\tau_z \\
&\quad +\gamma\eta[D_3 + (-\sin\phi\sin\theta k_y + \cos\theta k_z)k_x \\
&\quad + \cos\phi\sin\theta(k_y^2 + k_z^2)]\tau_y + \cdots,
\end{aligned} \tag{3}$$

where $m(\theta) = m - Be^2A_0^2\cos^2\theta$, $\gamma = -2B\lambda(eA_0)^2/\omega$, and $D_3 = -D_2Be^2A_0^2\sin^2\theta/(\gamma\omega)$.

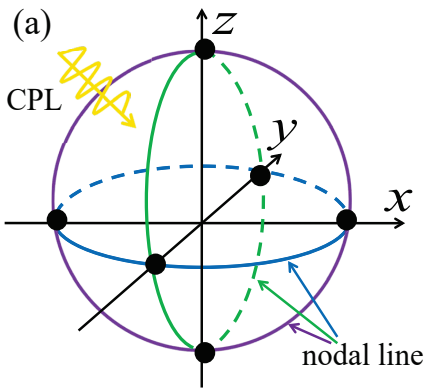

FIG. 1. Three nodal lines are located in three mutually orthogonal planes, and any two of them are mutually intersected.

II. CROSSING NODAL LINES WITH CUBIC SYMMETRY

The Hamiltonian for NLSMs with cubic symmetry is given by[1,2]

$$H(\mathbf{k}) = (m - Bk^2)\tau_x + \lambda k_x k_y k_z \tau_z. \tag{4}$$

The energy spectra read

$$E_\pm(\mathbf{k}) = \pm\sqrt{(m - Bk^2)^2 + (\lambda k_x k_y k_z)^2} \tag{5}$$

There are three nodal lines located in the three mutually perpendicular planes, respectively, i.e., the $k_x = 0$ plane, the $k_y = 0$ plane, and the $k_z = 0$ plane. Any two of the nodal lines mutually cross, as shown in Fig.1

Let us consider that the system is driven by a circularly polarized light with $\mathbf{A}(t) = A_0(\cos(\omega t)\mathbf{e}_1 + \eta\sin(\omega t)\mathbf{e}_2)$. The full time-periodic Hamiltonian can be expanded as $H(t, \mathbf{k}) = \sum_n H_n(\mathbf{k})e^{in\omega t}$ with

$$\begin{aligned}
H_0(\mathbf{k}) &= [m - Be^2A_0^2 - Bk^2]\tau_x + (\lambda k_x k_y k_z - G_1)\tau_z, \\
H_{\pm 1}(\vec{k}) &= -BeA_0[(\sin\phi k_x - \cos\phi k_y) \\
&\quad \mp i\eta(\cos\phi\cos\theta k_x + \sin\phi\cos\theta k_y - \sin\theta k_z)]\tau_x \\
&\quad +\lambda eA_0\{[(\sin\phi k_y k_z - \cos\phi k_x k_z) \mp i\eta(\cos\phi\cos\theta k_y k_z \\
&\quad + \sin\phi\cos\theta k_x k_z - \sin\theta k_x k_y)] + G_2 \pm iG_3\}\tau_z/2,
\end{aligned} \tag{6}$$

where

$$G_1 = \frac{\lambda(eA_0)^2}{4}(k_x\sin\phi\sin 2\theta + k_y\cos\phi\sin 2\theta + k_z\sin 2\phi\sin^2\theta),$$

$$G_2 = \frac{\lambda(eA_0)^3}{8}[2\cos^2\phi - \eta\cos 2\phi]\sin 2\theta,$$
$$G_3 = \frac{\eta\lambda(eA_0)^3}{8}[2\cos^2\theta\sin\theta - \sin^3\theta]\sin 2\phi. \quad (7)$$

All $H_{\pm n}$ with $n > 1$ will not be given explicitly because they contain only one pauli matrix τ_z, thus, they do not contribute to the effective Hamiltonian, which involves commutators. Following the approach in Eq.(3), we obtain the effective Hamiltonian:

$$\begin{aligned} H_{\rm eff}(\mathbf{k}) = &[\tilde{m} - Bk^2]\tau_x + (\lambda k_x k_y k_z - G_1)\tau_z \\ &+\gamma\eta[\cos\theta k_z(k_x^2 - k_y^2) + \sin\phi\sin\theta k_y(k_z^2 - k_x^2) \\ &+\cos\phi\sin\theta k_x(k_y^2 - k_z^2)]\tau_y + G_4\tau_y\cdots, \end{aligned} \quad (8)$$

where $\tilde{m} = m - Be^2A_0^2$, $\gamma = -2B\lambda(eA_0)^2/\omega$, and

$$\begin{aligned} G_4 = &\frac{2BeA_0}{\omega}[G_3(\sin\phi k_x - \cos\phi k_y) \\ &-\eta G_2(\cos\phi\cos\theta k_x + \sin\phi\cos\theta k_y - \sin\theta k_z)]. \end{aligned} \quad (9)$$

To simplify the discussion, we take into account the fact that $eA_0 << \sqrt{m/B}$, so that for a general incident direction, both G_1 and G_4 can be safely neglected. Under this approximation, the energy spectra read

$$\begin{aligned} E_\pm(\mathbf{k}) = \pm\{&(\tilde{m} - Bk^2)^2 + (\lambda k_x k_y k_z)^2 + \gamma^2[\cos\theta k_z(k_x^2 - k_y^2) \\ &+\sin\phi\sin\theta k_y(k_z^2 - k_x^2) + \cos\phi\sin\theta k_x(k_y^2 - k_z^2)]^2\}^{1/2}. \end{aligned} \quad (10)$$

It is readily found that there are six Floquet Weyl points when $\theta \neq 0, \pi$, or $\{\phi, \theta\} \neq \{\{0, \pi/2, \pi, 3\pi/2\}, \{\pi/2\}\}$,

$$\begin{aligned} \mathbf{Q}_1 = -\mathbf{Q}_2 &= \frac{\sqrt{\tilde{m}/B}}{\sqrt{(\sin\phi\sin\theta)^2 + \cos^2\theta}}(0, \sin\phi\sin\theta, \cos\theta), \\ \mathbf{Q}_3 = -\mathbf{Q}_4 &= \frac{\sqrt{\tilde{m}/B}}{\sqrt{(\cos\phi\sin\theta)^2 + \cos^2\theta}}(\cos\phi\sin\theta, 0, \cos\theta), \\ \mathbf{Q}_5 = -\mathbf{Q}_6 &= \sqrt{\tilde{m}/B}(\cos\phi, \sin\phi, 0), \end{aligned} \quad (11)$$

and their monopole charge are given by

$$C_1 = -C_2 = C_3 = -C_4 = C_5 = -C_6 = \eta. \quad (12)$$

When $\theta = 0$, π, or $\{\phi, \theta\} = \{\{0, \pi/2, \pi, 3\pi/2\}, \{\pi/2\}\}$, one of the three nodal lines remains, and the other two become a pair of double-Weyl points. For example, it is readily seen from Eq.(11) that when (ϕ, θ) is tuned to $(0, \pi/2)$, Q_3 and Q_5 (Q_4 and Q_6) will come close to each other; when (ϕ, θ) is tuned to $(\pi/2, \pi/2)$, Q_1 and Q_5 (Q_2 and Q_6) will come close to each other; when θ is tuned to 0 or π, Q_1 and Q_3 (Q_2 and Q_4) will come close to each other.

Without loss of generality, we consider the case $(\phi, \theta) = (0, \pi/2)$ to see the monopole combination. For this special case, both G_1 and G_4 are strictly equal to zero, and $H_{\rm eff}$ reduces to

$$H_{\rm eff} = [\tilde{m} - Bk^2]\tau_x + \lambda k_x k_y k_z\tau_z + \gamma\eta k_x(k_y^2 - k_z^2)\tau_y. \quad (13)$$

which gives two double-Weyl points at $Q_\pm = \pm(\sqrt{\tilde{m}/B}, 0, 0)$ with monopole charge

$$C_\pm = \pm 2\eta. \quad (14)$$

Besides the two double-Weyl points, $H_{\rm eff}$ also gives a nodal line which is located in the $k_x = 0$ plane and determined by $k_y^2 + k_z^2 = \tilde{m}/B$. The survival of this nodal line originates from the fact that the incident direction of the light is perpendicular to the plane in which the nodal line is located. The appearance of this additional nodal line does not affect the combination of Weyl points with the same monopole charge to form double-Weyl points.

III. SURFACE STATE EVOLUTION OF TYPE-II CROSSING

The effective Hamiltonian of the type-II crossing is given by (see Eq.(3))

$$\begin{aligned} H_{\rm eff}(\mathbf{k}) = &[m(\theta) - B(k_x^2 + k_y^2) + Bk_z^2]\tau_x + (\lambda k_y k_z - 2D_1)\tau_z \\ &+\gamma\eta[D_3 + (-\sin\phi\sin\theta k_y + \cos\theta k_z)k_x \\ &+\cos\phi\sin\theta(k_y^2 + k_z^2)]\tau_y. \end{aligned} \quad (15)$$

We consider that the system occupies the whole $z > 0$ region. Similar to the procedures in the main article, we neglect the D_1 term and D_3 term, and take the driving-induced τ_y term as a perturbation, i.e., $H_{\rm eff} \simeq H_0 + \Delta H$ with

$$\begin{aligned} H_0(\mathbf{k}) &= [m(\theta) - B(k_x^2 + k_y^2) + Bk_z^2]\tau_x + \lambda k_y k_z\tau_z \\ \Delta H(\mathbf{k}) &= \gamma\eta[(-\sin\phi\sin\theta k_y + \cos\theta k_z)k_x \\ &\quad +\cos\phi\sin\theta(k_y^2 + k_z^2)]\tau_y. \end{aligned} \quad (16)$$

Solving the eigenfunction $H_0(k_x, k_y, -i\partial_z)\Psi(x, y, z) = E_0(k_x, k_y)\Psi(x, y, z)$ under the boundary conditions $\Psi(z = 0) = 0$ and $\Psi(z \to +\infty) = 0$ gives $E_0 = 0$ and

$$\Psi(x, y, z) = \mathcal{N}e^{ik_x x}e^{ik_y y}(e^{-\kappa_+ z} - e^{-\kappa_- z})\chi \quad (17)$$

with $\chi = (sgn(k_y), i)^T/\sqrt{2}$ and

$$\kappa_\pm = \frac{\lambda|k_y|}{2B} \pm \frac{i}{2B}\sqrt{4B(\tilde{m}(\theta) - Bk_x^2 - Bk_y^2) - \lambda^2 k_y^2}, \quad (18)$$

The surface state exists only when $\min\{{\rm Re}\kappa_+, {\rm Re}\kappa_-\} > 0$. Here, $\mathcal{N}$ is a normalization constant, which takes the form of

$$\mathcal{N} = \begin{cases} \sqrt{-\frac{2\kappa_+\kappa_-(\kappa_+ + \kappa_-)}{(\kappa_+ - \kappa_-)^2}}, & \text{for } \kappa_+ = \kappa_-^*, \\ \sqrt{\frac{2\kappa_+\kappa_-(\kappa_+ + \kappa_-)}{(\kappa_+ - \kappa_-)^2}}, & \text{for } \kappa_\pm = \kappa_\pm^* \text{ and } \kappa_\pm > 0, \end{cases} \quad (19)$$

The modification to the energy dispersion of the surface states by ΔH is

$$\begin{aligned} \Delta E(k_x, k_y) &= \int_0^\infty dz\Psi^\dagger(x, y, z)\Delta H(k_x, k_y, -i\partial_z)\Psi(x, y, z) \\ &= -sgn(k_y)\gamma\eta[(\sin\phi\sin\theta k_x k_y - \cos\phi\sin\theta k_y^2) \\ &\quad -\kappa_+\kappa_-\cos\phi\sin\theta]. \end{aligned} \quad (20)$$

For $\theta = \pi/2$ and $\phi = 0$, namely, the angle corresponding to monopole annihilation, the energy dispersion is

$$E(k_x, k_y) = {\rm sgn}(k_y)\gamma\eta[\tilde{m}/B - k_x^2]. \quad (21)$$

For this angle, the surface state only exists in the regime $\tilde{m}/B > k_x^2 + k_y^2$. It is immediately seen that Fermi arc is absent at the Fermi energy $E_F = 0$, agreeing with the fact that monopoles have annihilated with each other at this angle.

IV. EFFECT OF SPIN-ORBIT COUPLING

A. Crossing nodal lines robust against spin-orbit coupling

When materials has certain symmetry, e.g., mirror symmetry or nonsymmorphic symmetry, nodal lines can stably exist even in the presence of spin-orbital coupling[3–5]. For instance, we assume that the crossing nodal lines are around a high symmetric point (most of the predicted materials fall into this class) and the low-energy effective Hamiltonian is given by

$$H(\mathbf{k}) = (m - Bk^2)\tau_x + \lambda k_x k_y k_z \tau_z + \lambda_{so}\tau_x\sigma_z, \qquad (22)$$

where λ_{so} denotes the spin-orbit coupling strength. For this type of spin-orbit coupling, it only induces a change of the size of the nodal lines, but does not destroy the crossing structure.

We consider that a CPL is incident in x direction and described by the vector potential $\mathbf{A} = A_0(0, \cos\omega t, \eta \sin\omega t)$. Following the same steps as in the main article, we obtain the effective Hamiltonian in the off-resonant regime, which is

$$H_{\text{eff}}(\mathbf{k}) = (m - Bk^2)\tau_x + \lambda k_x k_y k_z \tau_z + \lambda_{so}\tau_x\sigma_z + \gamma\eta k_x(k_y^2 - k_z^2)\tau_y. \qquad (23)$$

It is readily found that there are two pairs of double-Weyl points, with one pair located at $W_{1,\pm} = \pm(\sqrt{(\tilde{m} + \lambda_{so})/B}, 0, 0)$, and the other pair located at $W_{2,\pm} = \pm(\sqrt{(\tilde{m} - \lambda_{so})/B}, 0, 0)$. Thus, when the crossing-nodal-line structure are robust against the spin-orbit coupling, the double-Weyl points can still be dynamically created. The effect of spin-orbit coupling is to induce a shift of the positions of the Floquet Weyl points.

B. Crossing nodal lines not robust against spin-orbit coupling

The nodal lines in some of the predicted material candidates evolve into pairs of Dirac points in the presence of spin-orbit coupling. To describe this case, we consider a simplified model related to the crossing-nodal-line semimetal CaTe[6].

$$H(\mathbf{k}) = (m - Bk^2)\tau_x + \lambda k_x k_y k_z \tau_z\sigma_z + \lambda_{so}\tau_z(k_x\sigma_y - k_y\sigma_x) \qquad (24)$$

Without the spin-orbit coupling term, i.e., $\lambda_{so} = 0$, the Hamiltonian hosts three mutually orthogonal nodal lines. The presence of the spin-orbit coupling term will gap out the nodal lines, leaving only two Dirac points at $(0, 0, \pm\sqrt{m/B})$.

Now we also consider a CPL is incident in x direction and described by the vector potential $\mathbf{A} = A_0(0, \cos\omega t, \eta \sin\omega t)$. The effective Hamiltonian can be similarly obtained, which is

$$H_{\text{eff}}(\mathbf{k}) = (\tilde{m} - Bk^2)\tau_x + \lambda k_x k_y k_z \tau_z\sigma_z + \lambda_{so}\tau_z(k_x\sigma_y - k_y\sigma_x) + \gamma'\eta[2B\lambda k_x(k_y^2 - k_z^2)\tau_y\sigma_z + 2B\lambda_{so}k_z\tau_y\sigma_x + \lambda\lambda_{so}k_x k_y\sigma_y], \qquad (25)$$

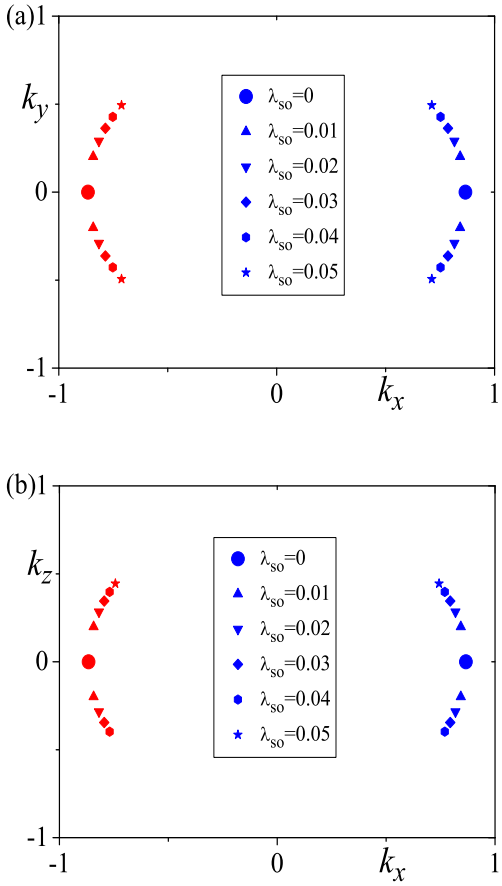

FIG. 2. The splitting of doubly-degenerate double-Weyl points into Weyl points in the presence of spin-orbit coupling. The parameters chosen for illustration are: $m = 1$, $B = 1$, $\lambda = 1$, $eA_0 = 0.5$, $\omega = 2$. (a) $k_z = 0$ plane. (b) $k_y = 0$ plane. The two filled dots mark the locations of the double-Weyl points in the absence of spin-orbit coupling, and other symbols denote the location of single-Weyl points in the presence of spin-orbit coupling. Red and blue color represent opposite monopole charges.

where $\gamma' = -(eA_0)^2/\omega$. When $\lambda_{so} = 0$, $H_{\text{eff}}(\mathbf{k})$ reduces to

$$H_{\text{eff}}(\mathbf{k}) = (\tilde{m} - Bk^2)\tau_x + \lambda k_x k_y k_z \tau_z\sigma_z + 2B\lambda\gamma'\eta k_x(k_y^2 - k_z^2)\tau_y\sigma_z,$$

which harbors a pair of doubly-degenerate double-Weyl points at $Q_\pm = \pm(\sqrt{\tilde{m}/B}, 0, 0)$. When $\lambda_{so} \neq 0$, the energy spectra of this Hamiltonian can not be analytically solved, thus we calculate it numerically. As shown in Fig.2, the pair of doubly-degenerate double-Weyl points are spilt into four pairs of Weyl points in the presence of weak spin-orbit coupling, with two pairs located at the $k_y = 0$ plane, and the other two pairs located at the $k_z = 0$ plane.

V. EXPERIMENTAL ESTIMATIONS

A. Estimation of the modification to energy bands

The modification to energy bands by the driving can be evaluated by calculating the quantity $|\gamma/\lambda| = 2Be^2A_0^2/\omega$, in which λ is the parameter of static Hamiltonian (see main article). As $A_0 = \mathcal{E}_0/\omega$, where $\mathcal{E}_0$ is the electric field strength, the quantity can be further rewritten as

$$|\frac{\gamma}{\lambda}| = \frac{2Be^2\mathcal{E}_0^2}{\omega^3}. \tag{26}$$

For ω and $\mathcal{E}_0$, we adopt the experimental parameters in the pump-probe experiment[7], where $\omega = 120$ meV, and $\mathcal{E}_0 = 2.5\times10^7$ V/m. For B, we take the material candidate Cu_3NPd to make an estimate. According to the band structure obtained by first principle calculation[1,2], $m \sim 0.5$ eV, and $\sqrt{m/B} \sim 0.2\pi/a$ with $a = 3.85$ Å[8], thus $B \sim 2\times10^{-19}$ eVm^2. Then

$$\begin{aligned}|\frac{\gamma}{\lambda}| &\sim \frac{2\times2\times10^{-19}eVm^2\times(2.5\times10^7V/m)^2}{(0.12eV)^3}\\ &\approx 0.14.\end{aligned} \tag{27}$$

Such a magnitude of modification can be readily observed in current experiments.

B. Estimation of Hall voltage in experiments

Due to the existence of monopole charges, anomalous Hall effect will show up in WSMs. At zero temperature and neutrality point (chemical potential $\mu = 0$), the Hall conductivities are given by[9]

$$\sigma_{\alpha\beta} = \frac{e^2}{h}\epsilon^{\alpha\beta\tau}\sum_i \frac{C_i k_\tau^{(i)}}{2\pi}, \tag{28}$$

where $\alpha,\beta,\tau = \{x,y,z\}$ and $\epsilon^{\alpha\beta\tau}$ is the Levi-Civita symbol; C_i and $k_\tau^{(i)}$ denotes the monopole charge and the τ-component of the momentum of the i-th Weyl point, respectively.

Now we consider the NLSM Hamiltonian with cubic symmetry (see Sec.II). For a CPL incident in a general direction $\mathbf{n} = (\cos\phi\sin\theta, \sin\phi\sin\theta, \cos\theta)$, the Hall conductivities can be obtained according to Eq.(28), which are

$$\begin{aligned}\sigma_{xy} &= \eta\frac{e^2}{h}\frac{\sqrt{\tilde{m}/B}}{\pi}\{\frac{\cos\theta[1-\delta_{\theta,\pi/2}(\delta_{\phi,0}+\delta_{\phi,\pi})]}{\sqrt{(\sin\phi\sin\theta)^2+\cos^2\theta}}\\ &+\frac{\cos\theta[1-\delta_{\theta,\pi/2}(\delta_{\phi,\pi/2}+\delta_{\phi,3\pi/2})]}{\sqrt{(\cos\phi\sin\theta)^2+\cos^2\theta}}\},\\ \sigma_{yz} &= \eta\frac{e^2}{h}\frac{\sqrt{\tilde{m}/B}}{\pi}\{\frac{\cos\phi\sin\theta[1-\delta_{\theta,\pi/2}(\delta_{\phi,\pi/2}+\delta_{\phi,3\pi/2})]}{\sqrt{(\cos\phi\sin\theta)^2+\cos^2\theta}}\\ &+\cos\phi(1-\delta_{\theta,0}-\delta_{\theta,\pi})\},\\ \sigma_{zx} &= \eta\frac{e^2}{h}\frac{\sqrt{\tilde{m}/B}}{\pi}\{\frac{\sin\phi\sin\theta[1-\delta_{\theta,\pi/2}(\delta_{\phi,0}+\delta_{\phi,\pi})]}{\sqrt{(\sin\phi\sin\theta)^2+\cos^2\theta}}\\ &+\sin\phi(1-\delta_{\theta,0}-\delta_{\theta,\pi})\}.\end{aligned} \tag{29}$$

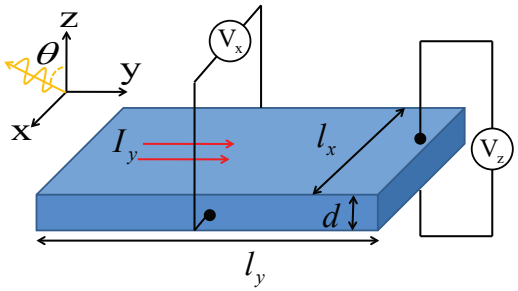

FIG. 3. Schematic picture of the experimental setup for the measurement of angle-dependent anomalous Hall effect. The CPL is incident in the x-z plane. I_y represents an electric current in the y direction, l_y denotes the spacing between current contacts. l_x and d denote the length in the x direction and the thickness in the z direction (also the spacing between voltage contacts). V_x and V_z are the Hall voltages to be measured.

Now we consider an experimental setup illustrated in Fig.3. In Fig.3, I_y represents the current in y direction and we will assume that it is distributed uniformly. l_y denotes the spacing between current contacts, while l_x and d denote the length in the x direction and the thickness in the z direction (also the spacing between voltage contacts). Because the current is in the y direction, σ_{zx} will play no role in transport, so we restrict the CPL in the x-z plane in which σ_{zx} naturally vanishes.

The resultant Hall voltage can be estimated as follows:

$$\begin{aligned}V_x &= R_{xy}I_y\\ &\approx -\frac{\sigma_{xy}\delta/d}{\sigma_{yy}^2+(\sigma_{xy}\delta/d)^2+(\sigma_{yz}\delta/l_x)^2}\times\frac{l_x}{l_y d}\times I_y,\\ V_z &= R_{zy}I_y\\ &\approx \frac{\sigma_{yz}\delta/l_x}{\sigma_{yy}^2+(\sigma_{xy}\delta/d)^2+(\sigma_{yz}\delta/l_x)^2}\times\frac{d}{l_x l_y}\times I_y.\end{aligned} \tag{30}$$

Here we have assumed that $\sigma_{xx} = \sigma_{yy} = \sigma_{zz}$ for simplicity as the original static system has cubic symmetry. δ is the penetration depth, determined by $\delta(\omega) = \frac{n(\omega)\epsilon_0 c}{\mathrm{Re}\sigma(\omega)}$, with $n(\omega)$ the refraction index of the material, ϵ_0 the permittivity of vacuum, c the speed of light, and $\mathrm{Re}\sigma(\omega)$ the absorption part of the optical conductivity, which only depends on the size of the nodal line, i.e., $\mathrm{Re}\sigma(\omega) = \frac{e^2}{h}\frac{\pi}{8}\sqrt{m/B}$. Due to the cubic symmetry of the original Hamiltonian, δ is also assumed to be isotropic.

In the following, we also take Cu_3NPd, a material candidate of NLSM with type-I crossing, as a concrete example to estimate the Hall conductivities and the Hall voltages. Cu_3NPd crystallizes in the cubic perovskite structure with lattice constant $a = 3.85$ Å[8]. First principle calculations found that the nodal-line size (diameter) is about $0.4\pi/a$, i.e., $\sqrt{m/B} \sim 0.2\pi/a$[1,2]. For $\theta = 0$, the angle that creates double-Weyl points, we have

$$\begin{aligned}|\sigma_{xy}| &= 2\frac{e^2}{h}\frac{\sqrt{\tilde{m}/B}}{\pi} \approx 4\times10^4\Omega^{-1}m^{-1},\\ \sigma_{yz} &= 0.\end{aligned} \tag{31}$$

We do not find any experimental result of the refractive index $n(\omega)$ of Cu_3NPd, but for its parent material Cu_3N, the refrac-

tive index $n(\omega)$ is about 3 in the visible light regime[10], and we take this value to estimate the penetration depth. Thus,

$$\delta(\omega) \approx \frac{n(\omega)\epsilon_0 c}{\pi^2 e^2/40ha}, \approx \frac{3\times 8.85\times 10^{-12}\times 3\times 10^8\times 40\times 6.63\times 10^{-34}}{3.14^2\times(1.6\times 10^{-19})^2}a, \approx 834a \approx 320nm. \quad (32)$$

For the dc conductivity of Cu_3NPd, the room temperature value[11] is about $1\times 10^5\Omega^{-1}m^{-1}$. The value in the zero temperature limit is expected to be larger, and we assume $\sigma_{yy} = 5\times 10^5\Omega^{-1}m^{-1}$ as an estimation. We take $l_x = l_y = 100\,\mu$m, $d = 500$ nm, and $I_y = 100$ mA, then a combination of Eq.(30), Eq.(31) and Eq.(32) gives $V_x \approx 20$ mV, which is well within the capacity of current experiments.

[1] Y. Kim, B. J. Wieder, C. L. Kane, and A. M. Rappe, Phys. Rev. Lett. **115**, 036806 (2015).

[2] R. Yu, H. Weng, Z. Fang, X. Dai, and X. Hu, Phys. Rev. Lett. **115**, 036807 (2015).

[3] G. Bian, T.-R. Chang, R. Sankar, S.-Y. Xu, H. Zheng, T. Neupert, C.-K. Chiu, S.-M. Huang, G. Chang, I. Belopolski, D. S. Sanchez, M. Neupane, N. Alidoust, C. Liu, B. Wang, C.-C. Lee, H.-T. Jeng, A. Bansil, F. Chou, H. Lin, and M. Zahid Hasan, Nature Communications **7**, 10556 (2016).

[4] G. Bian, T.-R. Chang, H. Zheng, S. Velury, S.-Y. Xu, T. Neupert, C.-K. Chiu, S.-M. Huang, D. S. Sanchez, I. Belopolski, N. Alidoust, P.-J. Chen, G. Chang, A. Bansil, H.-T. Jeng, H. Lin, and M. Z. Hasan, Phys. Rev. B **93**, 121113 (2016).

[5] T. Bzdušek, Q. Wu, A. Rüegg, M. Sigrist, and A. A. Soluyanov, Nature (London) **538**, 75 (2016), arXiv:1604.03112 [cond-mat.mes-hall].

[6] Y. Du, F. Tang, D. Wang, L. Sheng, E.-j. Kan, C.-G. Duan, S. Y. Savrasov, and X. Wan, npj Quantum Materials **2**, 3 (2017).

[7] Y. Wang, H. Steinberg, P. Jarillo-Herrero, and N. Gedik, Science **342**, 453 (2013).

[8] U. Hahn and W. Weber, Phys. Rev. B **53**, 12684 (1996).

[9] K.-Y. Yang, Y.-M. Lu, and Y. Ran, Phys. Rev. B **84**, 075129 (2011).

[10] I. Odeh, Journal of Alloys and Compounds **454**, 102 (2008).

[11] A. Ji, N. Lu, L. Gao, W. Zhang, L. Liao, and Z. Cao, Journal of Applied Physics **113**, 043705 (2013).